



Soft Lens Detection in Iris Image using Lens Boundary Analysis and Pattern Recognition Approach

Nur Ariffin Mohd Zin¹, Hishammuddin Asmuni², Haza Nuzly Abdull Hamed³

¹Faculty of Computer Science and Information Technology, Universiti Tun Hussein Onn Malaysia, Malaysia, ariffin@uthm.edu.my

²School of Computing, Faculty of Engineering, Universiti Teknologi Malaysia, Malaysia, hishamudin@utm.my

³School of Computing, Faculty of Engineering, Universiti Teknologi Malaysia, Malaysia, haza@utm.my

ABSTRACT

Recent studies have demonstrated that the soft lens wearing during iris recognition has indicated the increase of false reject rate. It denies the strong belief that the soft lens wearing will cause no performance degradation. Therefore, it is a necessity for an iris recognition system to be able to detect the presence of soft lens prior to iris recognition. As a first step towards soft lens detection, this study proposed a method for segmenting the soft lens boundary in iris images. However, segmenting the soft lens boundary is a very challenging task due to its marginal contrast. Besides, the flash lighting effect during the iris image enrolment has caused the image to suffer from inconsistent illumination. In addition, the visibility condition of the soft lens boundary may be discerned as a bright or dark ridge as a result of the flash lighting. Three image enhancement techniques were therefore proposed in order to enhance the contrast of the soft lens boundary and to provide an even distribution of intensities across the image. A method called summed-histogram has been incorporated as a solution to classify the visibility condition of the soft lens boundary automatically. The visibility condition of the ridge is used to determine the directional directive magnitude by the ridge detection algorithm. The proposed method was evaluated with Notre Dame Contact Lens Detection 2013 database. Results showed that the proposed method has successfully segment the soft lens boundary with an accuracy of over 92%.

Key words :Soft Lens Boundary Segmentation, Image Enhancement, Summed-Histogram, Iris Recognition.

1. INTRODUCTION

Iris holds a unique pattern amongst biological features in the human body [1], whereby stumbling between two identical iris is almost impossible. The iris texture begins to form as early as the third month of gestation and completely formed by eight of the months. As opposed to other biological features, the texture of the iris is stable over time, which is why it is being utilised in recognition system nowadays.

Furthermore, in comparison with other biometric modalities, iris recognition does not involve any physical contact [2].

Currently, detection of iris liveness has received a lot of concern in addressing countermeasure from spoofing attacks. The use of contact lenses has been identified as one way of spoofing [3]-[5]. This sort of threat utilises contact lens to imitate the pattern of one's iris to infringe a security system. Hence, for an iris recognition system to be extremely reliable, the capacity to sense spoofing attacks is essential for the system. In this situation, it is of utmost significance to detect and classify the existence and categories of contact lenses [6].

There are two types of contact lens, which are the cosmetic lens and soft lens (non-cosmetic lens). Cosmetic lenses are designed to alter the colour or visual appearance on one's eye. Meanwhile, a soft lens is worn to correct or improve eye vision. A cosmetic lens may available in a wide variety of colours while a soft lens is usually colourless. Besides, one could hardly tell if a person is wearing a soft lens unless being inspected carefully. Much attention has been gained to achieve accurate cosmetic lens detection; contrarily, less attention has been gained on soft lens detection. Nevertheless, it is still found to be a challenging task in order to achieve an accurate soft lens detection [7].

Literature has suggested four approaches of soft lens detection, which includes the hardware-based approach, lens boundary analysis approach, pattern recognition approach and deep learning approach [8]. The hardware-based approach requires the use of sophisticated devices in order to detect soft lenses. Reference [9] proposed the use of thermal cameras to measure the decrement of temperature on the eye surface during blinking to indicate soft lens wearing. Their approach has managed to achieve up to 72% of Correct Classification Rate (CCR). However, this approach is sensitive to the surrounding temperature and humidity as it affects the thermal cameras reading.

The lens boundary analysis approach deals with segmenting the soft lens boundary in iris images. Pioneering by [10], they attempted to examine the intensity profiles along the sclera

region for pixels with the largest intensity value that conform to the soft lens boundary. This approach has achieved up to 76% of CCR. However, the CCR is highly dependent on how accurate the soft lens boundary is segmented.

The most popular approach for soft lens detection is pattern recognition, which requires the combination of feature descriptor and classifier. Here, the feature descriptor is employed to extract the discriminative details of specific regions in iris images. Generally, discriminative details describe the principal characteristics such as texture, shape, gradient, colour, motion and others. The extracted discriminative details are used as training data by the classifier for classification. Various descriptors ranging from Scale-Invariant Feature Transform [11], Local Binary Pattern [6], Scale-Invariant Descriptor [12], Binarised Statistical Image Features [4], [13], [14] has been demonstrated. While Support Vector Machines has been used in [11]-[16], and other 14 different classifiers as in [6] has been used. Among of these, the one by [12] has achieved the highest CCR which is 89.88%. However, the classification performance is highly dependent on regions where the discriminative details are extracted.

The deep learning approach does not require the deployment of feature descriptor. Instead, it only works with a series of classifier called Convolutional Neural Network (CNN) trained with multiple patches of iris images of different variations. Related studies that implemented the deep learning approach for soft lens detection are such from [3] and [17]. As to date, the highest CCR of 89.58% has been achieved by [17]. The main drawback is CNN can be enormous in size as more convolutional layers are being implemented [18]. Thus, the deep learning approach is often computationally expensive.

In this study, we proposed the combination of lens boundary analysis approach and pattern recognition approach. The lens boundary analysis approach emphasises on segmenting the soft lens boundary while the pattern recognition approach carries the soft lenses detection. The opt for lens boundary analysis approach is based on three arguments. Firstly, it is inspired by the principle that the soft lens boundary is partly visible in the sclera region and statistically achievable to be detected [10]. Secondly, the utilisation of soft lens boundary is unaffected by types or manufacturers of the soft lens since it does not involve any visual texture like iris and cosmetic lens [19]. Thirdly, the resulted segmentation of the soft lens boundary provides more focused region for feature extraction, which tends to yield finer and more meaningful details [20]. Meanwhile, the implementation of pattern recognition approach compensates the parameters re-adjustment issue of lens boundary approach by adopting a machine learning mechanism that can adapt and predict the unforeseen data without the need of parameters re-adjustment. The next section discusses the issues in soft lenses detection.

2. PROBLEM BACKGROUND

The wearing of soft lens will leave a circular boundary on the sclera region as demonstrated in Figure 1. The soft lens boundary is barely distinguishable due to its nature that shares the same colour with the surrounding pixels while having different intensities. This condition might increase the probability of the soft lens boundary is being missed from the segmentation. Furthermore, the use of conventional edge detection might generate poor result as it only works by detecting any sharp changes between pixel intensities, whereas the soft lens boundary exhibits very marginal changes of pixel intensities [7]. The iris images also have the tendency to be exposed to inconsistent illumination, where one area tends to be brighter than to the other area, as shown in Figure 2. As a result, the changes of pixel intensities between these areas might be falsely segmented as the soft lens boundary. On the other hand, as a result of inconsistent illumination, the soft lens boundary may visible as a bright or dark ridge. This would require different parameters selection in order to yield an accurate segmentation. The succeeding section describes the proposed method to address the aforementioned issues.

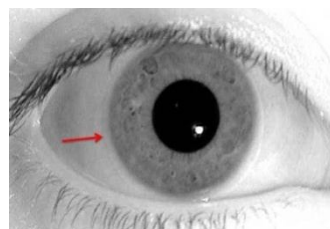


Figure 1: Visible circular boundary on the sclera region

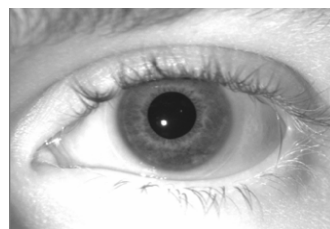


Figure 2: Inconsistent illumination across the eye

3. PROPOSED METHOD

The proposed method comprises soft lens boundary segmentation and soft lenses detection which executed in sequence. The segmentation consists of six steps as presented in Figure 3 while the detection is illustrated in Figure 4. The sub-sections onward explain every step in detail.

3.1 Image Enhancement

Image enhancement technique is applied to increase the contrast between the soft lens boundary and the sclera region. Apart from that, it works to normalise the pixel intensity across the region. In this study, three image enhancement techniques are evaluated which is Histogram Equalisation

(HE), Contrast Limited Adaptive Histogram Equalisation (CLAHE) and Homomorphic Filter (HF). Each of the technique is executed and evaluated separately, thus resulting in its corresponding enhanced image as visualised in Figure5.

3.2 Sclera Region Segmentation

This step involves the segmentation of both left and right sclera region from the resulted enhanced image. The segmentation is scaled down to the region that the soft lens boundary is deemed to reside. It begins with the iris segmentation to retrieve the outer boundary of the iris, which also corresponds to the border between iris and sclera. During this process, the iris radius (r_i) is obtained, which resulted in circular segmentation of iris. The iris segmentation reflects the concentric shape of sclera segmentation, where it shares the same centre with iris.

As suggested by [10], the sclera region takes another 30 pixels (r_s) from the iris radius (r_i) that uniform to the circular boundary of iris. Subsequently, the circular sclera region segmentation is cropped into two points of vector that represent the upper and lower boundaries of the segmented region, which is annotated as P_U and P_L respectively. The right sclera region is segmented between an upper value of 150 to lower value of 210 degrees (θ), while 30 to -30 (θ) degrees respectively at the left region. The use of upper and lower boundaries is inspired by [21] where it was initially utilised during iris normalisation in preparation for feature extraction. These values were empirically chosen to ensure minimum interference of noise such as eyelashes and eyelids. It also ensures maximum details of the soft lens boundary properties are being captured. Figure 6 shows the segmented sclera region marked as white regions.

3.3 Sclera Region Normalisation

The sclera region normalisation remaps each point of the segmented sclera region from Cartesian coordinate into polar coordinates using the Daugman’s rubber sheet model [22]. The original implementation has been modified for the mapping only covers the range between upper boundaries, P_U and lower boundaries, P_L . The normalised sclera region resulted from the mapping process is in a size of 30x240 pixels as shown in Figure7 (a) and 7 (b).

3.4 Eyelash Removal

The eyelash removal process is executed due to cases where the normalised sclera region tends to have remaining noises derived from eyelashes. For such condition, the highest possibility came from subjects which have longer eyelashes, hence occludes the sclera region. Commonly, the occlusion affects either left or right sclera region. Any segmented sclera region that indicates the presence of eyelashes is supposed to have black coloured artefacts in arbitrary shape across the normalised sclera region. The eyelashes may intrude the soft

lens segmentation process as it may be falsely detected as a soft lens boundary. Therefore, these eyelashes are removed using inpainting algorithm [23]. Inpainting algorithm is an image correction algorithm that purposely replaces the targeted object (eyelashes) pixels with surrounding pixels.

3.5 Summed-Histogram

Due to the flash lightings, the soft lens boundary may form as a bright or dark ridge. A bright ridge is apparent in a region where excessive brightness exists while dark ridge visible in normal illumination condition. These variations are shown in Table 1. Visible inspection shows that there was no case where both sides of the sclera encounter bright ridges. It is due to the nature that bright ridge always visible on one side of the sclera region due to the illumination from the flash lighting [10].

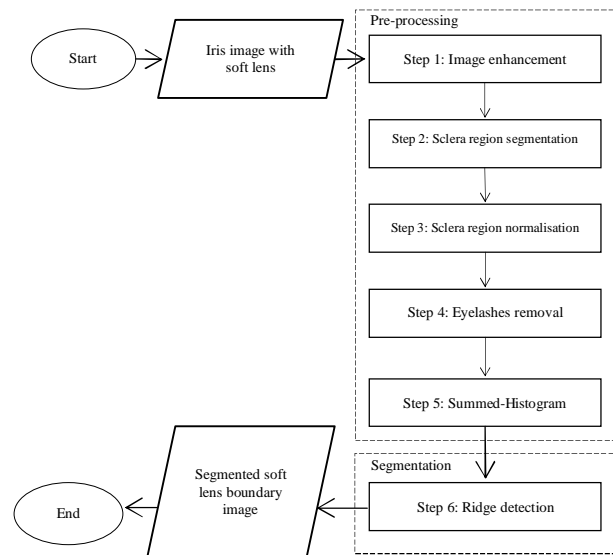


Figure 3: The steps of soft lens boundary segmentation

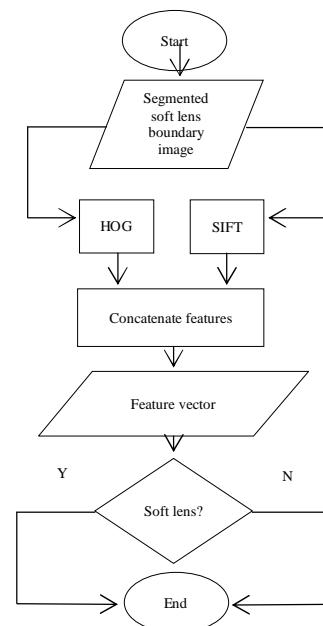


Figure4: The steps of soft lenses detection

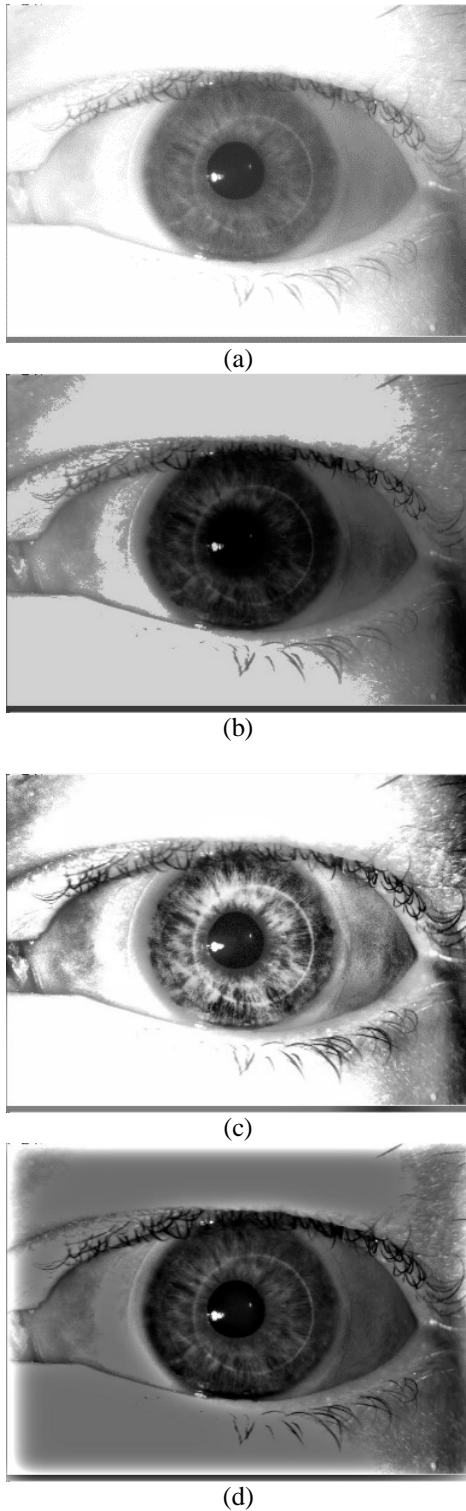


Figure5: The (a) original image of subject 04261 with its corresponding enhanced images, (b) from HE, (c) from CLAHE and (d) from HF

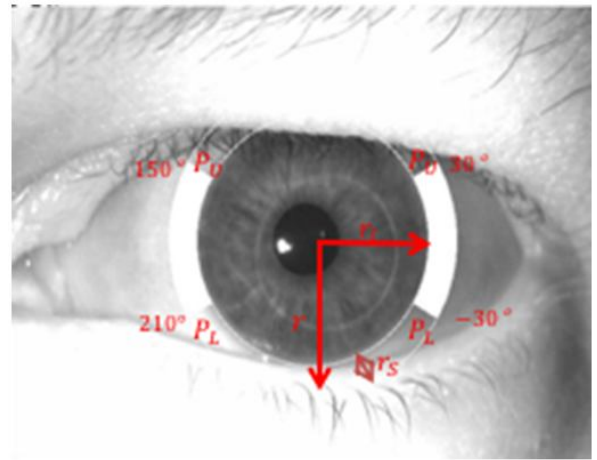


Figure 6: The white regions which mark the segmented sclera region

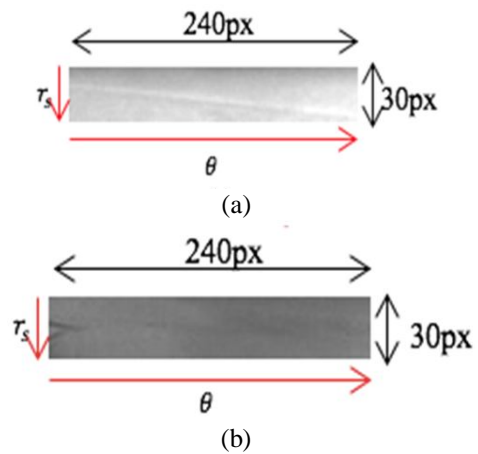


Figure7: The sclera region normalisation of (a) right and (b) left sclera region

Table 1: Variation of the visibility condition of the soft lens boundary on the left and right normalised sclera region

Subject	Iris image	Normalised sclera region	
		Left	Right
0426 1			
0539 2			

The primary purpose of summed-histogram is to provide an automatic classification of the visibility condition of the soft lens boundary, whether it is visible as bright or dark ridges. The visibility condition of the soft lens boundary is used as a

measurement to determine the directional directive magnitude for the ridge detection algorithm to recognise the directional change of intensities from dark to bright (bright ridge) and bright to dark (dark ridge).

By default, the ridge detection algorithm in step six of the proposed method does not have the ability to select the ridge condition automatically. Without summed-histogram, the directional directive magnitude is not optimised to the visibility condition of the soft lens boundary. The summed-histogram works by extracting both left and right normalised sclera region into 256 bins of grayscale histogram. Every bin in this histogram represents intensity value from 0 to 255, where it stores the occurrences of each intensity from the whole image. The product of the summed-histogram is the summation of these occurrences. For each left and right normalised sclera region, the summed-histogram is calculated and compared. The one that obtains higher sum value is considered to have a bright ridge while the one that obtains lower sum value is considered to have a dark ridge. The summed-histogram of individual normalised sclera region, S is represented in (1) as follows:

$$S_{I'(r,\theta)} = \int_{n=0}^{255} \sum P_{I'(r,\theta)_n} + P_{I'(r,\theta)_{n+1}} + P_{I'(r,\theta)_{n+\dots}} + P_{I'(r,\theta)_{n+255}} \quad (1)$$

where, P is the occurrence of the intensity values of the normalised sclera region $I'(r,\theta)$ and n is the index of histogram bin starting from 0 to 255. The sum value, S determines the visibility condition of the soft lens boundary in the left and right normalised sclera region, $I^L(r,\theta)$ and $I^R(r,\theta)$, whether it falls under bright or dark ridges. (2) and (3) denote the ridges classification:

$$I^L(r,\theta) = \begin{cases} \text{Bright} & \text{if } S_{I^L(r,\theta)}^L > S_{I^R(r,\theta)}^R \\ \text{Dark} & \text{if } S_{I^L(r,\theta)}^L < S_{I^R(r,\theta)}^R \\ \text{Dark} & \text{if } S_{I^L(r,\theta)}^L \approx S_{I^R(r,\theta)}^R \end{cases} \quad (2)$$

$$I^R(r,\theta) = \begin{cases} \text{Bright} & \text{if } S_{I^R(r,\theta)}^R > S_{I^L(r,\theta)}^L \\ \text{Dark} & \text{if } S_{I^R(r,\theta)}^R < S_{I^L(r,\theta)}^L \\ \text{Dark} & \text{if } S_{I^R(r,\theta)}^R \approx S_{I^L(r,\theta)}^L \end{cases} \quad (3)$$

where, S^L and S^R are the left and right normalised sclera region respectively. The soft lens boundary in the left normalised sclera region, $I^L(r,\theta)$ is considered as a bright ridge if it has larger sum value, $S_{I^L(r,\theta)}^L$, as compared to the sum value from the right normalised sclera region, $S_{I^R(r,\theta)}^R$ and vice versa. While the soft lens boundary in the right normalised sclera region, $I^R(r,\theta)$ is considered as bright ridge if it has larger sum value, $S_{I^R(r,\theta)}^R$, as compared to the sum value from the left normalised sclera region, $S_{I^L(r,\theta)}^L$ and vice versa. The soft lens

boundaries in both normalised sclera regions are considered to have dark ridge if $S_{I^L(r,\theta)}^L$ and $S_{I^R(r,\theta)}^R$ yield approximately the same summed value within the tolerance of 20 points as suggested by [24].

3.6 Ridge Detection

Once the visibility condition of the soft lens boundary is known, as for the last step, the soft lens boundary in both left and right normalised sclera regions is segmented using ridge detection algorithm. As mentioned earlier, detecting the soft lens boundary using conventional edge detection might be irrelevant since soft lens boundary is located in the vicinity where the foreground and background are sharing the same colour while having a different intensity. Hence, this condition validated that the soft lens boundary is well suited to be referred to as a ridge rather than an edge [20]. The ridge detection algorithm is applied at an image point of the normalised sclera region $I^L(r,\theta)$ and $I^R(r,\theta)$ by calculating the second order derivative of a Gaussian function [25] as denoted in (4):

$$G(x,y,\sigma) = \frac{1}{2\pi\sigma^2} e^{-\frac{(x^2+y^2)}{2\sigma^2}} \quad (4)$$

By taking its partial derivative in x gives $G(x)$ as in (5):

$$\frac{\delta G(x,y,\sigma)}{\delta x} = -\frac{x}{2\pi\sigma^4} e^{-\frac{(x^2+y^2)}{2\sigma^2}} \quad (5)$$

And convoluting second-order derivative matrix with $I^L(r,\theta)$ and $I^R(r,\theta)$, denoted as in (6):

$$\begin{bmatrix} \frac{\delta^2 G(r,\theta,\sigma)}{\delta^2 r} & \frac{\delta^2 G(r,\theta,\sigma)}{\delta^2 r\theta} \\ \frac{\delta^2 G(r,\theta,\sigma)}{\delta^2 r\theta} & \frac{\delta^2 G(r,\theta,\sigma)}{\delta^2 \theta} \end{bmatrix} \quad (6)$$

Then, applying to the local directional derivative magnitude operator, calculated using (7) and (8):

$$\delta_p = \sin\beta\delta_r - \cos\beta\delta_\theta \quad (7)$$

$$\delta_q = \cos\beta\delta_r + \sin\beta\delta_\theta \quad (8)$$

where, p and q are coordinates of the rotated coordinate system of scale-space representation L . The determination of second-order directional derivative magnitude in p and q direction, L_{pq} is determined by (9):

$$L_{pq} = \begin{cases} L_{pq} < 0 & \text{if } I'(r,\theta) \in \text{Bright} \\ L_{pq} > 0 & \text{if } I'(r,\theta) \in \text{Dark} \end{cases} \quad (9)$$

where, L_{pq} will be in negative magnitude if the summed-histogram, $I'(r,\theta)$ correspond to a bright ridge while

L_{pq} will be in positive magnitude if the summed-histogram, $I^L(r, \theta)$ correspond to a dark ridge. The directional derivative magnitude L_{pq} that represent the segmented soft lens boundary is overlaid on the normalised sclera region images, $I^L(r, \theta)$ and $I^R(r, \theta)$ in the form of binary images. The segmented soft lens boundary is represented as logical 1s (white) while the sclera region represented as logical 0s (black).

Once the segmentation is completed, the detection steps are carried out. To actualise the use of a more focused region, the segmented soft lens boundary is employed for feature extraction. The features are extracted independently using two feature descriptors namely Histogram of Oriented Gradients (HOG) and Scale-Invariant Feature Transform (SIFT). The feature vectors resulted from each feature descriptor are concatenated. These concatenated feature vectors are used to train a model by employing Support Vector Machines (SVM). Finally, the model is used to classify whether an iris image is belong to with or without soft lens.

4. EXPERIMENTAL SETUP

The proposed method was evaluated with Notre Dame Contact Lens Detection 2013 (NDCLD13) database. This database provides three classes of iris images of without lenses, with soft lenses and with cosmetic lenses in the format of grayscale images. Every class has 1000 images in total. However, only soft lenses and without soft lenses images were used in this study. For every image in this class, ground truth images of the ideal soft lens boundary segmentation were prepared. The soft lens boundary was rendered manually using an image editing software, Paint.NET. Some samples of the ground truth images are shown in Table 2. The manually rendered soft lens boundary is marked as red colour. For each normalised sclera region image, the overlapping pixels between the ideal segmentation of the soft lens boundary (red pixels) and the segmented soft lens boundary resulted from the proposed method were calculated. In preparation for logical comparison, the ground truth images were binarised where the ideal segmentation of the soft lens boundary will be regarded as logical 1s (white colour), while background pixels (sclera region) as logical 0s (black colour). Then, pixels that fall under True Positive (TP), True Negative (TN), False Positive (FP) and False Negative (FN) were counted. The true positive score reflects how many pixels were correctly segmented as the soft lens boundary, while the true negative score reflects the non-soft lens boundary pixels that were correctly marked. False positive score refers to pixels that were incorrectly segmented as the soft lens boundary, while false negative score refers to the non-soft lens boundary pixels that were incorrectly marked.

Table 2: Samples of normalised sclera regions with their corresponding ground truth images

Subject	Normalised sclera region	Ground truth image
04261		
05682		
05828		
06136		

Subsequently, the sensitivity, specificity and accuracy scores were calculated as the following Equation (10), Equation (11) and Equation (12):

$$Sensitivity = \frac{TP}{TP + FN} \tag{10}$$

$$Specificity = \frac{TN}{TN + FN} \tag{11}$$

$$Accuracy = \frac{TN + TP}{TP + TN + FP + FN} \tag{12}$$

Six experiments were conducted, where each experiment differs in image enhancement applied, listed as HE, CLAHE and HF. The first three experiments utilised every image enhancement without the application of summed-histogram and the last three experiments combined every image enhancement with the application of summed-histogram. Each experiment was executed with 1000 iris images with the presence of soft lenses.

4. RESULTS AND ANALYSIS

The results of the experiments are presented in Table 3. Without the application of summed-histogram, HE has resulted in the lowest true positive score. With CLAHE, the score increased over 86%, leaving it in a huge score gap. HF stands out by resulting in the highest true positive score, with an increase over 17% from CLAHE. As for the true negative score, HE has maintained the lowest, followed by CLAHE with over 3% increment from HE. The HF has achieved the highest true negative score with over 5% increment from CLAHE. With the application of summed-histogram, the true positive and true negative score from HE has increased over 24 and 7% respectively. An increase of 9 and 6% has been achieved for the respective true positive and true negative score from CLAHE. Meanwhile, HF has resulted in 4% increment of true positive score and 3% increment of true negative score.

Table 3: Experimental results

Image enhancements		Sclera region	Percentage (%)			
			TP	TN	FP	FN
W/o summed-histogram	HE	Left	0.38	73.18	21.50	4.94
		Right	0.48	73.79	20.94	4.79
	CLAHE	Left	0.62	75.20	19.49	4.70
		Right	0.90	75.66	19.06	4.38
	HF	Left	0.72	78.39	16.30	4.60
		Right	1.05	79.63	15.09	4.22
With summed-histogram	HE	Left	0.47	77.82	16.87	4.85
		Right	0.57	79.27	15.45	4.70
	CLAHE	Left	0.67	79.55	15.13	4.64
		Right	0.95	80.04	14.69	4.32
	HF	Left	0.75	80.60	14.04	4.61
		Right	1.06	80.79	13.97	4.17

In overall, the application of HF has yielded better segmentation of the soft lens boundary by having higher true positive and true negative scores, as well as maintaining the lowest false positive and false negative scores. On the other hand, the implementation of summed-histogram has boosted up the segmentation performance by increasing the true positive and true negative scores while lowering false positive and false negative scores. It is also observed that the right sclera region resulted in a higher true positive and true negative score as compared to the left sclera region. It is due to the right sclera region possesses better contrast compared to the left sclera region as the flash lighting is more exposed to the right side of the iris image. Hence, the soft lens boundary is more distinguishable in order to be segmented. Meanwhile, the left sclera region consistently has lower true positive and true negative scores. It reflects the condition where the left sclera region has a lesser light source, leaving it in a low contrast condition, thus, causing the visibility of the soft lens boundary is less distinguishable.

Table 4 reported the sensitivity, specificity and accuracy between each image enhancement applied. In this study, sensitivity is expected to be lower than specificity as the soft lens boundary covers only a small proportion of the whole iris image. Among these three image enhancement techniques, HF has resulted in the highest sensitivity score which is 0.14 for the left sclera region and 0.20 for the right sclera region on both with and without the application of summed-histogram. HF again has achieved the highest specificity score, with 0.83 for left sclera region and 0.84 for right sclera region and achieved 0.85 for both sclera region with the application of summed-histogram. Without the application of summed-histogram, HF has achieved the highest accuracy among the other two image enhancement techniques. On the other hand, the application of summed-histogram has boosted up the accuracy to 81 and 82% for the left and right sclera region respectively.

Table 5 shows a sample result of the segmented soft lens boundary for an image which is among the best condition,

in which the visibility of the soft lens boundary is discernible without any blur. Among the three image enhancement techniques applied, the application of HF has resulted in the closest segmentation of the soft lens boundary. Meanwhile, the noises are lesser as compared to the other two image enhancement techniques. In this case, noises are regarded as points that are not connected with the segmented soft lens boundary trail and not representing the soft lens boundary at all. Noises also considered as points that deviated from the soft lens boundary trail. These noises are generated from the uneven distribution of intensities as a result of poor image enhancement.

Based on the visual comparisons, the combination of HF and summed-histogram has resulted in a more accurate segmentation and produced lesser noises. Based on the results presented in Table 3 and 4, there are a few interesting findings that can be discussed. The first finding is related to the three image enhancement techniques applied as contrast enhancement. In theory, HE improves global contrast throughout the image. This condition has caused the transition from dark to the bright area has been regarded as a misleading segmentation. As a result, the use of HE has shown poor segmentation performance. CLAHE, on the other hand operates on local contrast selection rather than global contrast selection. The use of clip limit in CLAHE aids in minimising over-amplification on bright and dark areas of the image. It was able to enhance the details of the soft lens boundary; however, the intensities distribution was still significantly uneven. It is because CLAHE enhances the local intensities at an equal level where unnecessary details appeared, which triggering false segmentation. Consequently, the implementation of CLAHE was unable to accomplish accurate soft lens segmentation. Meanwhile, HF works on global contrast selection, with the ability to separate illumination and reflectance into the frequency domain. Hence, HF did not over-enhance the intensities and the intensities distribution was evenly spread. Therefore, a more accurate segmentation has been achieved.

Table 4: The sensitivity, specificity and accuracy results of the segmentation

Image enhancements		Sclera region	Sensitivity	Specificity	Accuracy (%)
W/o summed-histogram	HE	Left	0.07	0.77	74
		Right	0.09	0.78	74
	CLAHE	Left	0.12	0.79	76
		Right	0.17	0.80	77
	HF	Left	0.14	0.83	79
		Right	0.20	0.84	81
With summed-histogram	HE	Left	0.09	0.82	78
		Right	0.11	0.84	80
	CLAHE	Left	0.13	0.84	80
		Right	0.18	0.84	81
	HF	Left	0.14	0.85	81
		Right	0.20	0.85	82

Table 5: The visual comparisons of segmented soft lens boundary for every image enhancement technique applied for subject 04261

Image enhancements		Sclera region	
		Left	Right
Ground truth			
W/o summed-histogram	HE		
	CLAHE		
	HF		
With summed-histogram	HE		
	CLAHE		
	HF		

The second finding relates to how effective the application of summed-histogram with every image enhancement technique applied. Based on the result presented in Table 4, the application of summed-histogram with HE has improved the segmentation accuracy up to 9%. In the meantime, with CLAHE, the segmentation accuracy has increased up to 6% while HF only achieved up to 3% increment. This trend shows that the application of summed-histogram has managed to significantly improve the segmentation accuracy of HE and CLAHE more, as compared to HF. Since HE and CLAHE are histogram based, the summed-histogram has provided a more distinctive set of values apart from their existing histogram bins. As the existing histogram bins only cater on splitting the intensities frequencies into a number of bins, summed-histogram provides the additional information on the intensity values that correspond to the bright or dark ridges in both left and right normalised sclera regions.

Finally, comparisons were made with the existing state of the arts, which distinguished by the regions for feature extraction as well as the various feature descriptors applied as presented in Table 6. The classification annotation for the samples of without soft lens is referred to as N, while the samples of with soft lens are referred to as S. N-N refers to the probability of without soft lens samples are classified belongs to without soft lens, while S-S refers to the probability of with soft lens samples are classified belongs to with soft lens. Based on the comparisons presented in Table 6, the proposed soft lens detection delivered the highest average Correct Classification Rate (CCR), gaining over 3% increment from its closest competitor which is from [16]. From the results, it is proven that the region for feature extraction plays a definitive role in generating better CCR. For N-N classification, the utilisation of whole image as region for feature extraction by [17] has achieved good result, which is 91.67%. Meanwhile, the proposed method has resulted in 6% increment from [17],

followed by [16] with 4% increment. For S-S classification, the proposed method has obtained the highest CCR which is 87.56%. However, the application of whole image by [17] has surpassed the employment of iris and sclera by [16], by having 4% increment. The main reason behind this is the application of multiple convolutional layers where each layer is assigned to analyse specific details, generating more intrinsic and interpretative content. Nevertheless, the approach of concatenating HOG and SIFT has yielded competitive result by providing global and local gradient occurrences with lesser outliers through the segmented soft lens boundary region. As similar to concatenation of SIFT and LBP and PHOG, by [5] the results of S-S classification have improved as compared to a single modified LBP. It is deemed that their results could be better if more focused region is applied as implemented by [16].

Table 6: Comparisons between the proposed soft lens detection and state of the arts

Feature descriptor	Region	N-N	S-S	Average CCR (%)
SIFT+LBP [5]	Pupil, iris, sclera	70.00	60.15	65.08
LBP+PHOG [5]	Pupil, iris, sclera	81.25	65.41	73.33
Modified LBP [5]	Pupil, iris, sclera	85.50	45.25	65.38
CNN [3]	Whole image	84.50	73.75	79.13
BSIF[14]	Whole image, iris and strip region	76.50	84.50	80.50
SID [16]	Iris, sclera	95.75	84.00	89.88
CNN [17]	Whole image	91.67	87.50	89.58
HOG+SIFT (Proposed)	Segmented lens boundary	96.80	87.56	92.18

5. CONCLUSION

This study proposed a method to detect soft lenses in iris images by the fusion of lens boundary analysis and pattern recognition approach. The lens boundary analysis focuses on the soft lens boundary segmentation while the pattern recognition carries the soft lenses detection. During the segmentation, three image enhancement techniques have been evaluated to enhance the contrast of the soft lens boundary and to provide an even intensity distribution across the image. A method named summed-histogram was implemented to provide automatic classification of the visibility condition of the soft lens boundary. From the experiments conducted, the implementation of HF was able to increase the contrast of the soft lens boundary by resulting a segmentation accuracy of 81%. Meanwhile, the addition of summed-histogram has increased the segmentation accuracy by resulting 9% increase with HE, a 6% increase with CLAHE and 3% increase with HF. As for the detection, the segmented soft lens boundary was used as the region for feature extraction using two feature descriptors, namely Histogram of Oriented Gradients (HOG) and Scale-Invariant Feature Transform (SIFT). Experimental results have shown

that the proposed soft lens detection has achieved the average CCR of 92%, which rated among the highest as compared to other state of the arts.

ACKNOWLEDGEMENT

Authors would like to thank Universiti Tun Hussein Onn Malaysia, UniversitiTeknologi Malaysia and Ministry of Higher Education Malaysia for providing fund and scholarship for this study.

REFERENCES

1. J.G.Daugman. **How iris recognition works**,*IEEE Transactions on Circuits and Systems for Video Technology*, Vol. 14, No. 1, pp. 21–30, Jan. 2004.
2. A.K.Jain, A.Ross, and S.Prabhakar. **An introduction to biometric recognition**,*IEEE Transactions on Circuits and Systems for Video Technology*, Vol. 14, No. 1, pp. 4–20, Jan. 2004.
3. P.Silva,E.Luz, R.Baeta, H.Pedrini, A.X.Falcao, and D.Menotti.**An approach to iris contact lens detection based on deep image representations**,in *2015 28th SIBGRAPI Conference on Graphics, Patterns and Images*, Salvador, Brazil, 2015, pp. 157–164.
4. J.S.Doyle, and K.W.Bowyer.**Robust detection of textured contact lenses in iris recognition using BSIF**,*IEEE Access*, Vol. 3, pp. 1672–1683. Sept. 2015.
5. D.Yadav, N.Kohli, J.S.Doyle, R.Singh, M.Vatsa, and K.W.Bowyer.**Unraveling the effect of textured contact lenses on iris recognition**,*IEEE Transactions on Information Forensics and Security*, Vo. 9, No. 5, pp. 851–862. March 2014.
6. J.S.Doyle, P.J.Flynn, and K.W.Bowyer. **Automated classification of contact lens type in iris images**,in *2013 International Conference on Biometrics (ICB)*, Madrid, Spain, 2013, pp. 1–6.
7. S.E.Baker, A.Hentz, K.W.Bowyer, and P.J.Flynn. **Degradation of iris recognition performance due to non-cosmetic prescription contact lenses**,*Computer Vision and Image Understanding*, Vol. 114, No. 9, pp. 1030–1044. Sept. 2010.
8. J.Galbally and M. Gomez-Barrero.**A review of iris anti-spoofing**,in *2016 4th International Conference on Biometrics and Forensics*, Limassol, Cyprus, 2016, pp. 1–6.
9. W.W.Kywe, M.Yoshida, and K.Murakami.**Contact lens extraction by using thermo-vision**, in*18th International Conference on Pattern Recognition (ICPR'06)*, Hong Kong, China, 2006, pp. 570–573.
10. G.Erdogan and A.Ross. **Automatic detection of non-cosmetic soft contact lenses in ocular images**, in*SPIE Biometric and Surveillance Technology for Human and Activity Identification X*, Baltimore, Maryland, United States.2013, p. 87120C.
11. H.Zhang, Z.Sun, and T.Tan. **Contact lens detection based on weighted LBP**,in *2010 20th International Conference on Pattern Recognition*, Istanbul, Turkey, 2010, pp. 4279–4282.
12. D.Graghaniello, G.Poggi, C.Sansone, and L.Verdoliva. **Contact lens detection and classification in iris images through scale invariant descriptor**, in*2014 10th International Conference on Signal-Image Technology and Internet-Based Systems*, Marrakech, Morocco, 2014, pp. 560–565.
13. J.Komulainen, A.Hadid, and M.Pietikainen. **Generalized textured contact lens detection by extracting BSIF description from cartesian iris images**,in *IEEE International Joint Conference on Biometrics*, Clearwater, Florida, United States, 2014, pp. 1–7.
14. R.Raghavendra, K.B.Raja, and C.Busch. **Ensemble of statistically independent filters for robust contact lens detection in iris images**, in*Proceedings of the 2014 Indian Conference on Computer Vision Graphics and Image Processing*, Bangalore, India, 2014, pp. 1–7.
15. N.Kohli, D.Yadav, M.Vatsa, and R.Singh.**Revisiting iris recognition with color cosmetic contact lenses**, in*2013 International Conference on Biometrics (ICB)*, Madrid, Spain, 2013, pp. 1–7.
16. D.Graghaniello, G.Poggi, C.Sansone, and L.Verdoliva. **Using iris and sclera for detection and classification of contact lenses**,*Pattern Recognition Letters*, Vol. 82, pp. 251–257. Oct. 2016.
17. A.Singh, V.Mistry, D.Yadav, and A.Nigam. **GHCLNet: A generalized hierarchically tuned contact lens detection network**. in*2018 IEEE 4th International Conference on Identity, Security, and Behavior Analysis (ISBA)*, Singapore, 2018, pp. 1–8.
18. M. M.Najafabadi, F.Villanustre, T. M.Khoshgoftaar, N.Seliya, R.Wald, and E.Muharemagic. **Deep learning applications and challenges in big data analytics**,*Journal of Big Data*, Vol. 2, No. 1, pp. 1-21, Dec. 2015.
19. B.Kumar, A.Nigam, and P.Gupta.**Automated soft contact lens detection using gradient based information**,in *11th Joint Conference on Computer Vision, Imaging and Computer Graphics Theory and Applications (VISIGRAPP 2016)*,Rome, Italy, 2016, pp. 358–365.
20. L.Chen, M.Jiang, and J.X.Chen. **Image segmentation using iterative watershed plus ridge detection**, in*2009 16th IEEE International Conference on Image Processing (ICIP)*, Cairo, Egypt, 2009, pp. 4033–4036.

21. G.Sathish. **Multi-algorithmic iris recognition**, *International Journal of Computer Applications*, Vol. 38, No. 11, pp. 13–21, 2012.
22. J.G. Daugman. **Biometric personal identification system based on iris analysis**, *U.S. Patent 5,291,560*, March 1994.
23. M.Bertalmio, G.Sapiro, V.Caselles, and C.Ballester. **Image inpainting**, in *Proceedings of the 27th Annual Conference on Computer Graphics and Interactive Techniques*. New Orleans, LA, United States, 2000, pp. 417–424.
24. R.Mehta and K.Egiazarian. **Dominant rotated local binary patterns (DRLBP) for texture classification**, *Pattern Recognition Letters*, Vol. 71, pp. 16–22, Feb. 2016.
25. T.Lindeberg. **Edge detection and ridge detection with automatic scale selection**, *International Journal of Computer Vision*, Vol. 30, No. 2, pp. 117–156, Nov. 1998.